The Japan Society of Mechanical Engineers

Bulletin of JSME, Vol. 29, No. 257 November 1986

Paper No. 257-6

An Evaluation of the Fracture Resistance of a Stably Growing Crack by Crack Energy Density (2nd Report, Application to a Ductile Crack in Thin Plate)*

Katsuhiko WATANABE** Hideyuki AZEGAMI*** Yasuo Hirano†

The method proposed in the 1st Report for evaluating the fracture resistance of a stably growing crack by crack energy density is applied to the stable crack growth problems of thin plates, and its applicability and validity are confirmed. Experiments of stable growth fractures are carried out for thin single-edge cracked specimens with different initial crack lengths under bending moment and thin center cracked specimens with different initial crack lengths under tensile force. The fracture resistances expressed by additional rates of crack energy density and crack energy density are evaluated, based on the results. When fracture modes are almost the same, fracture resistances have almost the same values regardless of initial crack lengths, and their values vary only corresponding to the change of fracture mode caused by crack extension. The difference of specimen types has no influence either on their values.

Key Words : Fracture, Thin Plate, Stable Crack Growth, Fracture Resistance, Crack Energy Density, Additional Rate of Crack Energy Density

1. Introduction

When the fracture resistance of a stably growing crack in a ductile material under monotonous load can be expressed by a crack parameter of which the physical meaning is clear, consistently from the initiation of crack growth to the last unstable fracture; and when it is confirmed that the value of the fracture resistance depends on the fracture mode, we can regard this fracture resistance as a characteristic value of the material and, based on this fracture resistance, we can evaluate the behavior of a stably growing crack in an actual structure. The crack energy density[1][2] is expected to be such crack parameter as described above, and this serial strudy purports to propose an evaluation method of fracture resistance by the crack energy density and prove the validity and applicability of the method through its applications to actual problems. In the 1st Report[3], we proposed a method to evaluate the fracture resistance of a stably growing crack by the crack energy density only from the relations between load, growing crack length, load-point-displacement and initial crack length which are easily measured through experiments. In this report, the authors try to apply the method to stably growing cracks in thin plates, that is, they evaluate the fracture resistances by the crack energy density based on the experiments of stable crack growths of thin plates and examine the correspondences between the fracture resistances obtained and the fracture modes observed and the influences of the specimen shapes and the loading modes.

* Received 1st May, 1985.

** Associate professor, Institute of Industrial Science, University of Tokyo, 7-22-1, Roppongi, Minato-ku, Tokyo, 106 Japan.

*** Research assistant, Toyohashi University of Technology, Hibarigaoka, 1-1, Tempaku-cho, Toyohashi-city, 440 Japan.

† Technical staff, Institute of Industrial Science, University of Tokyo.

2. Evaluation Method of Fracture Resistance

The evaluation method of fracture resistance proposed in the 1st Report is as described in the following.

When we consider a cracked plate with initial crack length a_0 which is loaded from the time $\tau=0$ and in which a crack begins to grow at the time $\tau=t_0$, the crack energy density at the crack tip $\mathcal{E}(t, a_0)$ at the time $\tau=t(\leqq t_0)$ before the onset of crack growth and the additional rate of crack energy density at the crack tip $\partial\mathcal{E}/\partial a(t, a)$ at the time $\tau=t(\geqq t_0)$ caused by stable crack growth are given by

$$\mathcal{E}(t, a_0)=-\frac{1}{B}\int_0^{u(t)}\frac{\partial P}{\partial a_0}(a_0, u)du \quad \cdots\cdots(1)$$

$$\frac{\partial\mathcal{E}}{\partial a}(t, a)=-\frac{1}{B}\frac{\partial P}{\partial a_0}(a_0, u)\Big/\left\{\frac{\partial a}{\partial u}(a_0, u)\cdot\frac{\partial a}{\partial a_0}(a_0, u)\right\} \quad \cdots\cdots(2)$$

respectively, where B is the thickness, and $P(a_0, u)$ and $a(a_0, u)$ are the load and the growing crack length, respectively, for the specimen with initial crack length a_0 at the time when the load-point-displacement is $u(\tau)$ (which corresponds one-to-one to the time τ). Therefore, through ex-

NII-Electronic Library Service

The Japan Society of Mechanical Engineers

Table 1 Chemical composition of material

THICKNESS	Si	Fe	Cu	Mn	Mg	Cr
mm	%	%	%	%	%	%
2.0	0.14	0.20	4.48	0.54	1.40	0.02

Zn	Tr+Ti	Ti	OTHERS EACH	OTHERS TOTAL	Al
%	%	%	%	%	
0.03	0.03	0.02	0.00	0.00	RE

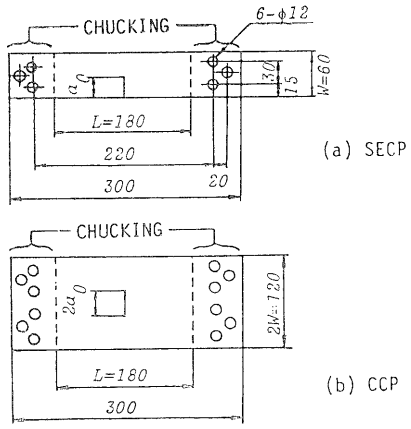

Fig.1 Geometries of Specimens

periments of stable crack growths in specimens with several initial crack lengths, the fracture resistances of $\mathcal{E}_c(t_0, a_0)$ and $\partial\mathcal{E}_c/\partial a(t, a)$ (which are expressed by adding subscript c in a sense of critical values as material properties and agree with the values determined based on the mechanical conditions in the process of stable crack growth) are evaluated by Eqs.(1) and (2). Furthermore, from the relations

$$\mathcal{E}(t, a)=\mathcal{E}(t_0, a_0)+\int_{t_0}^{t}\frac{d\mathcal{E}}{da}(\tau, a)\dot{a}d\tau \quad \cdots(3)$$

$$\frac{d\mathcal{E}}{da}(\tau, a)=\frac{1}{\dot{a}}\frac{d\mathcal{E}}{d\tau}(\tau, a)$$
$$=\frac{\partial\mathcal{E}}{\partial a}(\tau, a)+\frac{\partial\mathcal{E}}{\partial X_1}(\tau, a) \quad \cdots\cdots\cdots(4)$$

the fracture resistance of $\mathcal{E}_c(t, a)$ is also evaluated by using $\mathcal{E}_c(t_0, a_0)$ and $\partial\mathcal{E}_c/\partial a(t, a)$ and by putting a suitable value for $\partial\mathcal{E}_c/\partial X_1(\tau, a)$, where $\dot{(\ )}=\partial(\ )/\partial\tau$.

In this paper, the experiments of ductile crack stable growths of thin plates are carried out and the fracture resistances of $\mathcal{E}_c(t_0, a_0)$, $\partial\mathcal{E}_c/\partial a(t, a)$ and $\mathcal{E}_c(t, a)$ are evaluated in the above-mentioned manner. In the evaluation of $\mathcal{E}_c(t, a)$, considering that $d\mathcal{E}_c/da(\tau, a)=0$ or $\partial\mathcal{E}_c/\partial X_1(\tau, a)=-(\partial\mathcal{E}_c/\partial a)_{uni}$ (=const.) in the process of crack growth accompanied with a uniform fracture mode, $\partial\mathcal{E}_c/\partial a(\tau, a)=(\partial\mathcal{E}_c/\partial a)_{uni}$ is used (refer to Eq.(4)).

3. Experiment of Ductile Crack Stable Growth of Thin Plate

The method for the experiments on the ductile crack stable growths of thin plates and the results of the measurements on the

Table 2 Mechanical properties of material

THICKNESS	0.2% PROOF STRESS	TENSILE STRENGTH	ELONGATION
mm	GPa	GPa	%
2.0	0.327	0.470	22.0

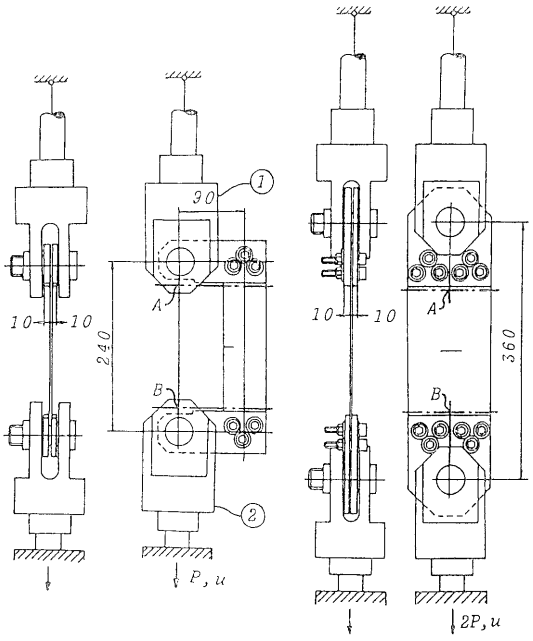

Fig.2 Specimens under load

relations between load, growing crack length, load-point-displacement and initial crack length which are required to evaluate $\mathcal{E}_c(t_0, a_0)$ and $\partial\mathcal{E}_c/\partial a(t, a)$ by Eqs.(1) and (2) are shown in this chapter. Here, thin plates are used to rapidly realize a crack growth accompanied with the uniform fracture mode of shear type and make the measurement of the growing crack length easy.

3.1 Experimental method

A thin plate, 2 mm in thickness, of aluminum alloy 2024-T3 was prepared for the experiments. Its chemical composition and mechanical properties are shown in Tables 1 and 2 respectively. Two types of specimens shown in Fig.1, single-edge-cracked-panel (SECP) and center-cracked-panel (CCP), were prepared and loaded as shown in Fig.2 to examine the influences of geometry of specimen and loading condition. As to the initial crack length a_0, six kinds of rates to the width W (refer to Fig.1), a_0/W = 0.1, 0.2, 0.3, 0.4, 0.5 and 0.6, were chosen. Incidentally, all the specimens are cut out so that the directions of cracks coincide with the L-T direction (the cracked planes are perpendicular to the roll direction).

The configuration of initial crack is shown in Fig.3 and every pre-fatigue crack is finished under cyclic load corresponding to the maximum stress intensity factor $K_{I\,max}$ = 0.25 KN/mm$^{3/2}$ in the states of CCP, SECP

NII-Electronic Library Service

The Japan Society of Mechanical Engineers

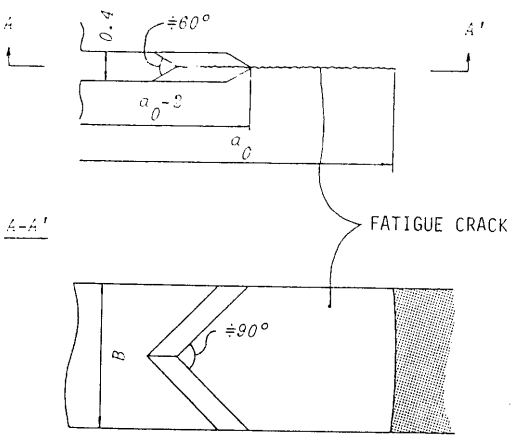

Fig.3 Configuration of initial crack

specimens were prepared by cutting off CCP after having finished pre-fatigue cracks. Here, the value of crack energy density equivalent to $K_{I\max}$ under plane stress condition is about 20 percent of the fracture resistance $\mathcal{E}_c(t_0, a_0)$ shown later.

The experiments were carried out by using an Instron type testing machine (10 tons in load capacity) as shown in Fig.4. The relative velocities between the crosshead and the screw rods were 0.5 mm/min for SECP and 0.1 mm/min for CCP. The stiffness of the testing machine was approximately estimated at 45 KN/mm based on the relation between the load and the displacement obtained by subtracting the load-point-displacement from the relative displacement between the crosshead and the screw rods.

In the case of SECP, the load P the growing crack length a and the load-point-displacement u were measured in the following manner. The load was measured by a load-cell (1 ton in full-scale) set on the upper part in Fig.4(a). The growing crack length was measured by counting the pulses on a recording chart of load and load-point-displacement. The crack tip was observed by a microscope and the pulses were recorded by turning a switch on at the moments when the crack tip had just moved across the grids printed at intervals of 0.5 mm on the surface of the specimen by Moire technique before the preparation of an initial crack. The load-point-displacement, which was defined as the relative displacement between the intersecting points A and B of the loading line and the dashed lines along the ends of the specimen in Fig.2(a), was measured by a differential transformer displacement gauge (±12.5 mm in full-scale, ① in Fig. 4(a)). The displacement gauge was supported by pins located at A and B and the pins were supported by arms (② and ③ in Fig.4(a)) fixed on the specimen by means of claws along the dashed lines. Further, the guideways made of Teflon and inlaid in the parts ① and ② in Fig.2(a) were prepared so that the pins could be located on the loading line. Moreover, in the experiment the following contrivances were provided. Buckling of the specimen was prevented by holding the specimen between

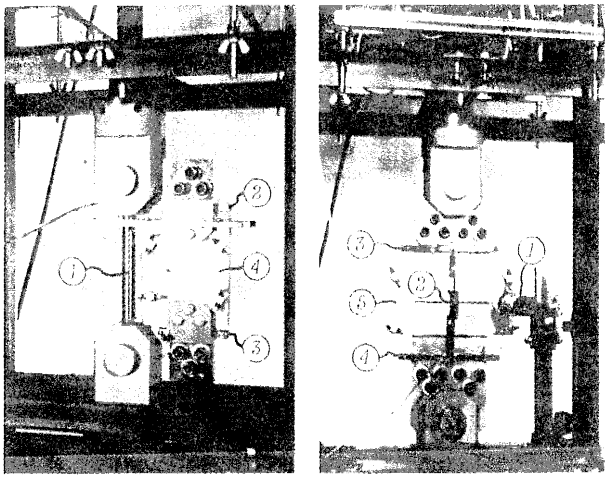

(a) SECP (b) CCP

Fig.4 Experimental configuration

side boards (④ in Fig.4(a)). The surface of the side board contacting with the specimen was greased and steel balls (2 mm is diamiter) were spread on it. The boards were suspended by wires hanging on bars attached to the upper part in Fig.2(a), so they could slide on the specimen when it was pulled down. The friction force between the side boards and the specimen was approximately estimated by measuring the maximum friction force by strain gauges stuck on the bars and its value was less than 0.04 KN. Furthermore, as the testing machine was a vertical type, a shear force was generated in the cracked plane because of the dead loads of specimen, chuck jig and displacement gauge. In order to elimnate this effect, the centers of gravity for upper and lower halves of the bodies were connected by a wire. The wire was hung on pulleys suspended by movable pulleys, which in turn were suspended by wires connecting the upper part with the tops of pillars fixed on the lower part. Thus, if the dead loads are just supported by the wire before loading, they are always cancelled.

On the other hand, in the case of CCP, the load P (actual load is $2P$, refer to Fig.2(b)) was measured by a load-cell (10 tons in full-scale) set on the upper part in Fig.4(b), and the growing crack length a (actual length is $2a$) was measured in the same way as in the case of SECP through the observation of the crack tip by means of microscope (① in Fig.4(b)). The load-point-displacement u, which is defined as the relative displacement between the points A and B in Fig.2(b), was measured by a displacement gauge of pi-type (0.5 mm in full-scale, ② in Fig.4(b)). The displacement gauge was supported by jigs (③ and ④ in Fig.4(b)) fixed on the specimen by means of claws along the dashed lines in Fig.2(b). Also in this expriment, buckling of the specimen was prevented by side boards (⑤ in Fig.4(b)). The friction force between the boards and the specimen was estimated in the same way as in the case of SECP and its value was less than 0.04 KN.

NII-Electronic Library Service

The Japan Society of Mechanical Engineers

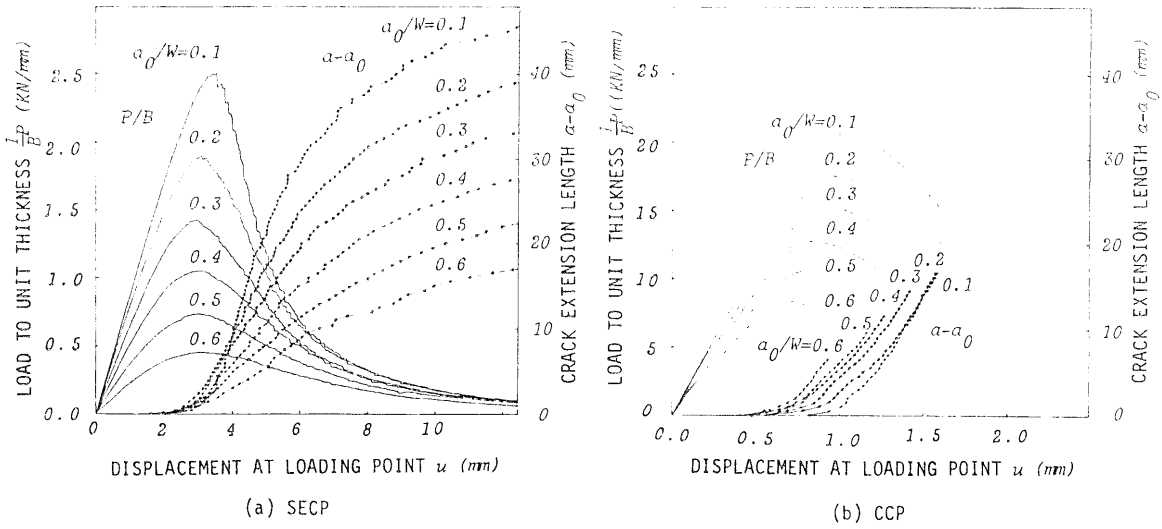

Fig.5 Results of load, crack growth length and load-point-displacement measurement

3.2 Results of measurements

Figure 5 presents the measured results of load per unit thickness P/B, crack growth length $a-a_0$ and load-point-displacement u for the specimens with six kinds of initial crack lengths a_0.

Unstable crack growth did not occur in the case of SECP, where a decreasing rate of load with load-point-displacement $-dP/du$ was smaller than the stiffness of testing machine. But it occurred, in the case of CCP, at the time when $-dP/du$ came close to the stiffness of the testing machine.

Figure 6 shows photographs of post-fracture surfaces taken from a perpendicular direction to the plate surfaces. In the photographs, the white parts are slant fracture surfaces inclined at 45 degrees to the plate surface. From the figure, it can be judged that the fracture mode change was hardly affected by the initial crack length, the shape of specimen and the loading condition. The fracture mode at the beginnning of crack growth was plane-strain type mainly caused by tear fracture. After the crack growth of 4 ∿ 8 mm length, crack growth accompanied with a uniform fracture mode of plane-stress type occurred.

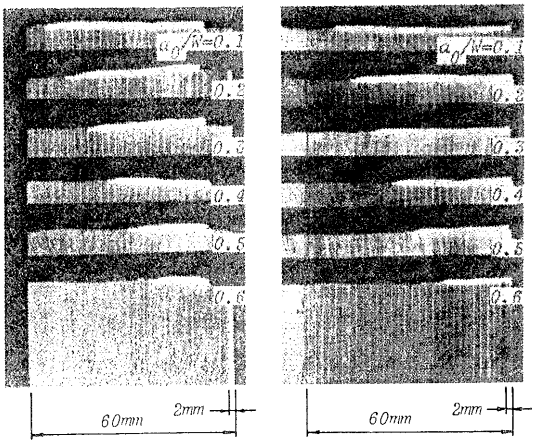

Fig.6 Photographs of post-fracture surfaces taken from perpendicular direction to plate

4. Evaluation of Fracture Resistance of Ductil Crack in Thin Plate

In this chapter, the fracture resistances of ductile cracks in thin plates expressed by the crack energy density are evaluated based on the results obtained in the previous chapter, and the correspondence between the fracture resistance and the fracture mode and the influences of configuration of specimen and loading condition are discussed.

4.1 Evaluations of $\mathcal{E}_c(t_0, a_0)$ and $\partial\mathcal{E}_c/\partial a(t, a)$

In this section, we evaluate the crack energy density at crack tip $\mathcal{E}_c(t_0, a_0)$ before the onset of crack growth and the additional rate of crack energy density at crack tip $\partial\mathcal{E}_c/\partial a(t, a)$ by Eqs.(1) and (2).

The results of measurements in the previous chapter are considered to be affected by minute discontinuous crack growth, scattering of configuration of the specimen including the initial crack length, scattering of fitness between the specimen and the jigs, and so forth. Accordingly, the load P and the growing crack length a were assumed to be the functions of the initial crack length a_0 and the load-point-displacement u expressed by $P(a_0, u)$ and $a(a_0, u)$ as done in the derivations of Eqs.(1) and (2), and their smoothed functions were obtained by the method of least squares and some corrections of the measurement results to avoid local fluctuations of partial-differential coefficients. The results are shown in Figs.7 and 8. Here, the smoothed functions are sets of the double-third-order B-spline functions[4], which are defined in

NII-Electronic Library Service

The Japan Society of Mechanical Engineers

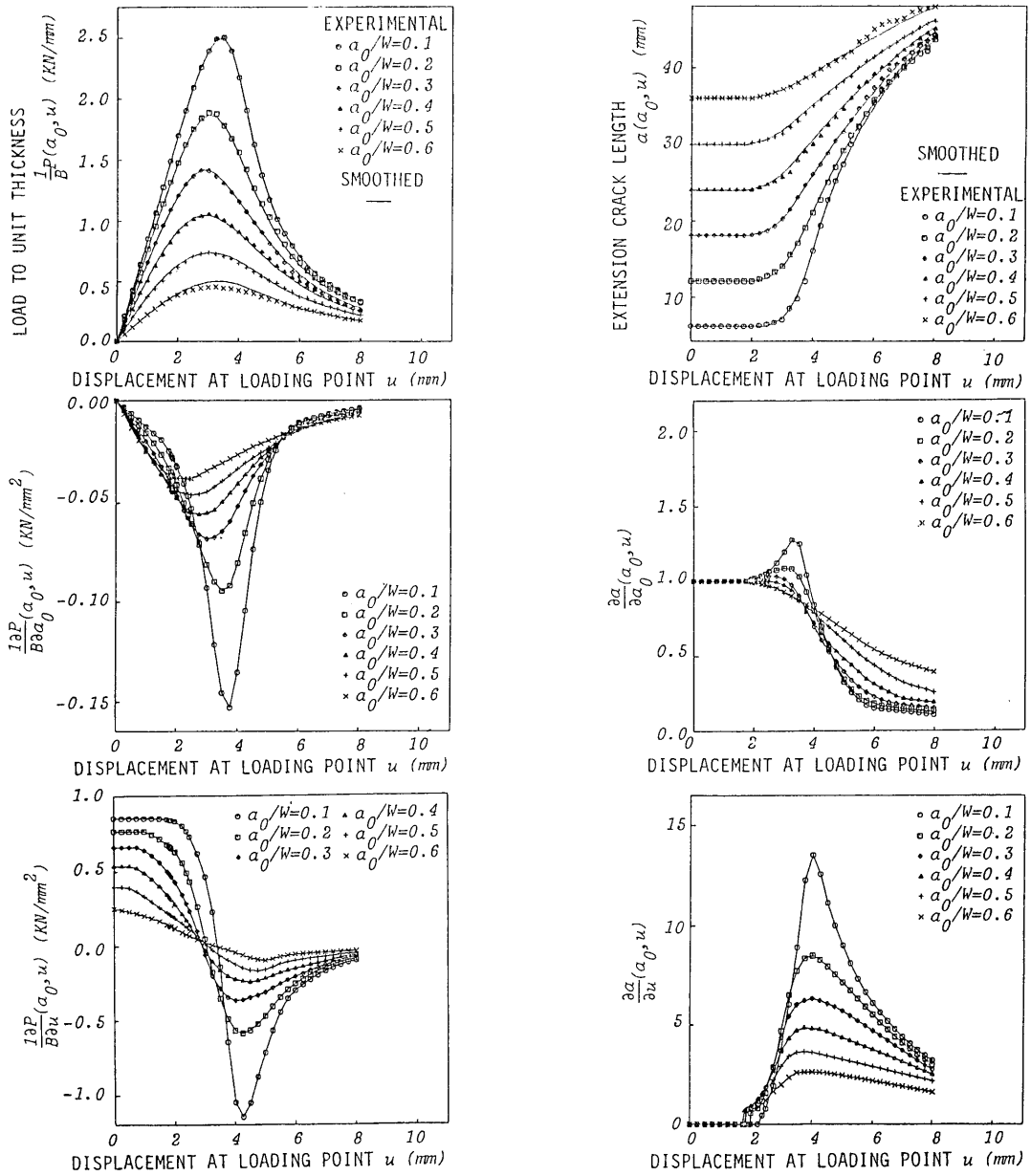

Fig.7 Smoothed results of $P(a_0, u)$ and $a(a_0, u)$ and their partial derivatives (SECP)

each rectangular partition divided at appropriate nodes of a_0 and u and they satisfy the continuities of the second derivatives in the whole region. Incidentally, in the case of CCP, there is a region on the a_0-u plane where the measurement results were not obtained because of an unstable crack growth. In the region, extrapolated values, which do not disturb the partial-derivatives evaluated in the part where the measurement results are obtained, are substituted. Further, if the variational rate of growing crack length with load-point-displacement at the onset of crack growth has a finite positive value except zero, the partial-differential coefficient of growing crack length with load-point-displacement becomes discontinuous at the onset of crack growth. In this case, after putting a smaller value than initial crack length into the growing crack length before the onset of crack growth and evaluating the partial-differential coefficient, we substitute the value of initial crack length for the growing crack before the onset of crack growth.

$\mathcal{E}_c(t, a_0)$ and $\partial\mathcal{E}_c/\partial a(t, a)$ evaluated from Eqs.(1) and (2) respectively by using the smoothed relations of $P(a_0, u)$ and $a(a_0, u)$ and their partial-differential coefficients are shown in Figs.9 and 10. In Fig. 9, the maximum point for each initial crack length corresponds to the onset of crack growth. From the results in Figs.9 and 10, we can say as follows;

(i) The results of $\mathcal{E}_c(t_0, a_0)$ are independent of the initial crack length, and their values seem to be peculiar to the specimen types.

(ii) The results of $\partial\mathcal{E}_c/\partial a(t, a)$ are also

NII-Electronic Library Service

The Japan Society of Mechanical Engineers

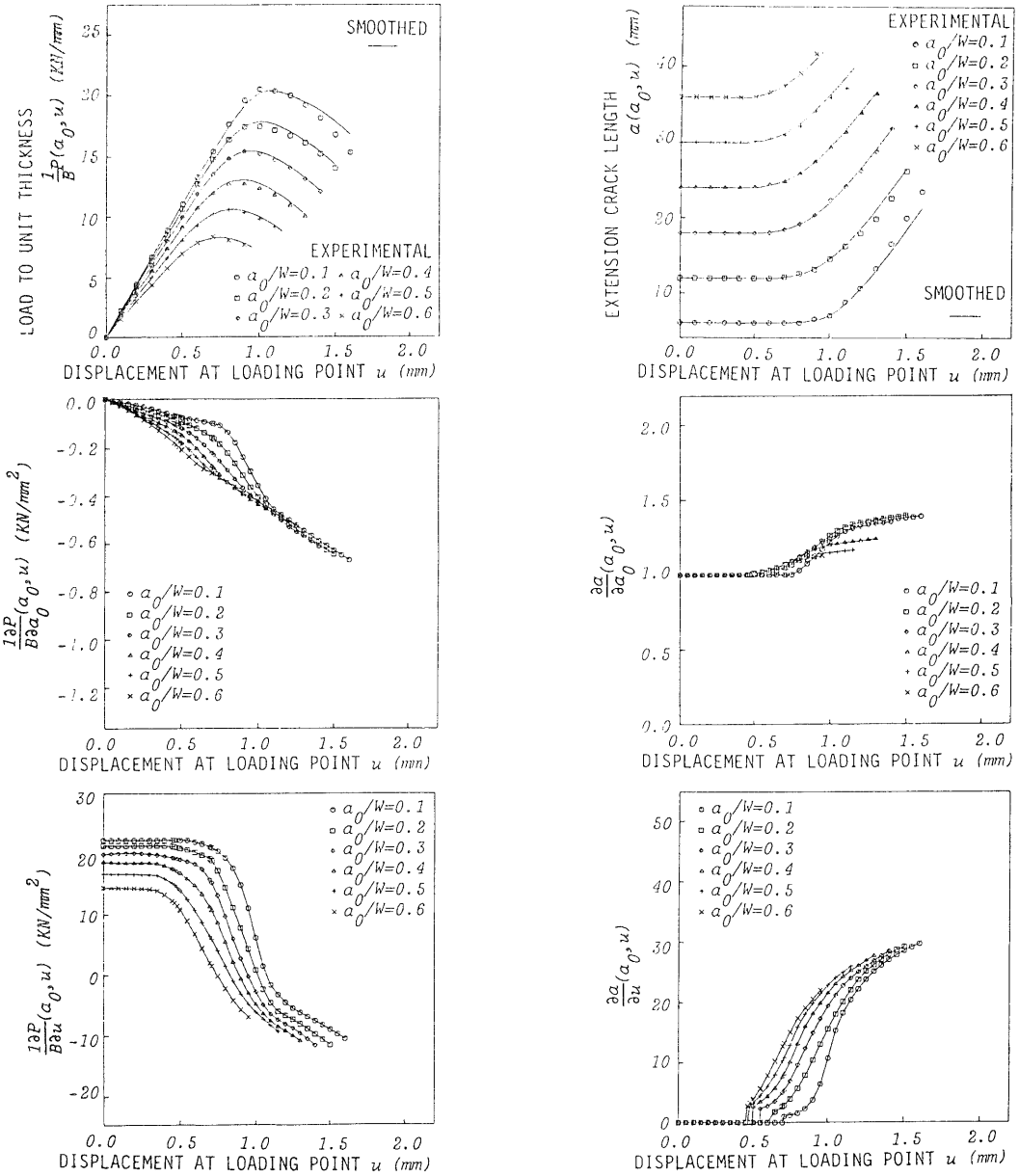

Fig.8 Smoothed results of $P(a_0, u)$ and $a(a_0, u)$ and their partial derivatives (CCP)

independent of the initial crack lengths, and their changes seem to be peculiar to the specimen types. Further, the changes correspond to the changes of the shape of post-fracture surface, and their values become constant in the region of the crack growth accompanied with a uniform fracture mode as predicted in chapter 2.

We represent the characteristic values in (i) by $\mathcal{E}_{c\,tear}$ because they seem to mainly correspond to the mode of tear fracture through the ovservations of post-fracture surfaces (refer to Fig.6), and the constant values in (ii) by $(\partial\mathcal{E}_c/\partial a)_{shear}$ because they correspond to the mode of shear fracture. The results for two specimen types obtained as the averages of the values for each initial crack length are shown in Table 3. From the table, we can judge as follows;

(iii) The value of $\mathcal{E}_{c\,tear}$ is scarcely affected by the configuration of specimen and the loading condition.
(iv) The value of $(\partial\mathcal{E}_c/\partial a)_{shear}$ for CCP is slightly larger than that for SECP.

The tendency in (iv) is grasped as follows. The distribution of stresses on the ligament plane for SECP changes on a large scale from tension to compression and, on the other hand, that for CCP changes on a small scale under tension comparatively. Therefore, the histories of deformations until fracture are different for the two specimen types and this difference affects the fracture mode of the specimen. Based on the results and considerations, it can be said that the values of $\mathcal{E}_c(t_0, a_0)$ and $\partial\mathcal{E}_c/\partial a(t, a)$ are the characteristic values of the material corresponding to fracture mode and the evaluation of

NII-Electronic Library Service

The Japan Society of Mechanical Engineers

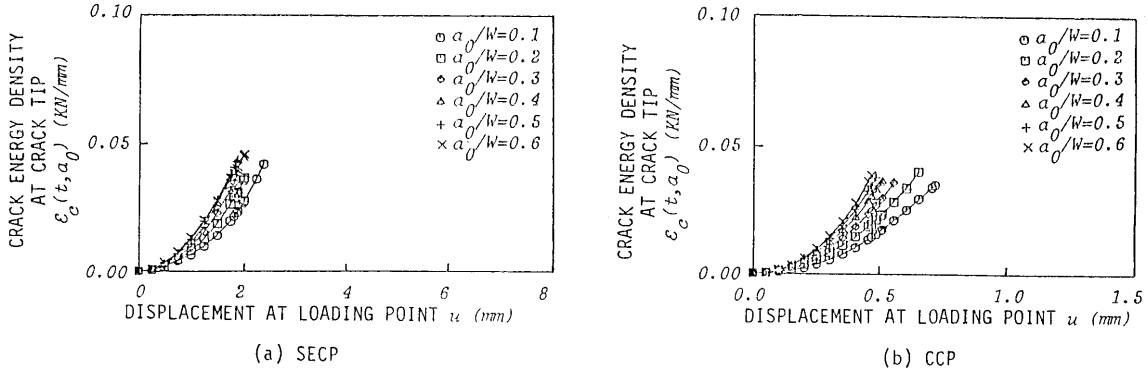

Fig.9 Crack energy densities at ctack tip $\mathcal{E}(t, a_0)$ before onset of crack growth

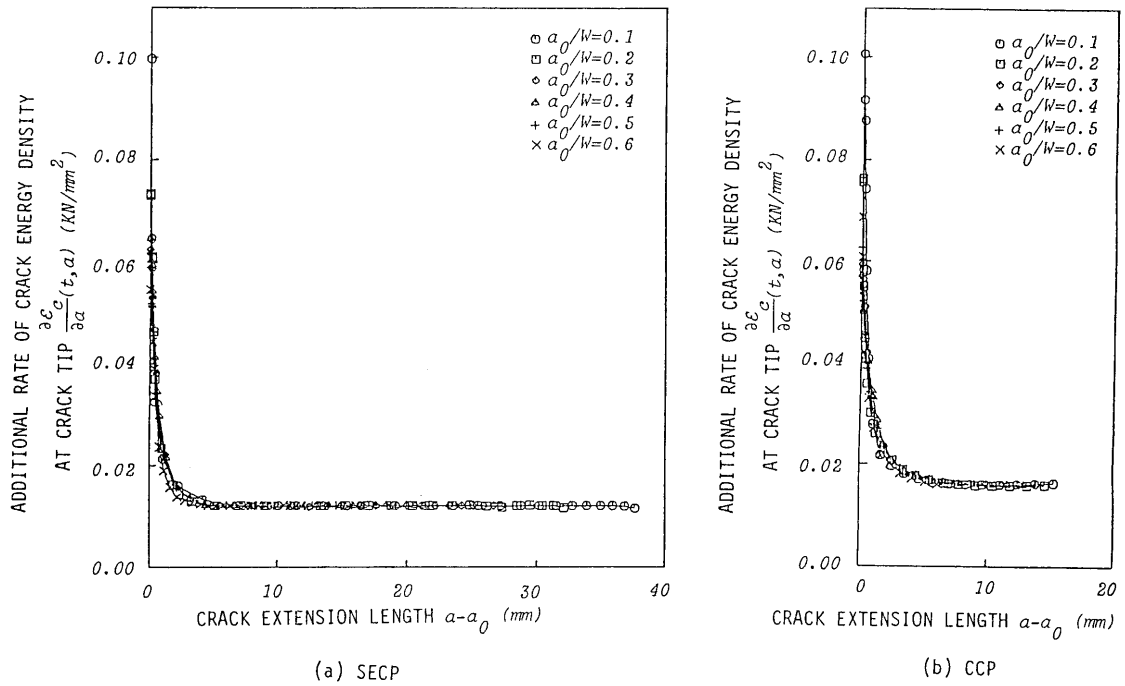

Fig.10 Additional rates of crack energy density at crack tip with crack growth

fracture resistance by the combination of $\mathcal{E}_c(t_0, a_0)$ and $\partial \mathcal{E}_c/\partial a(t, a)$ is valid and available.

4.2 Evaluation of $\mathcal{E}_c(t, a)$

In this section, we evaluate the crack energy density at crack tip $\mathcal{E}_c(t, a)$ after the onset of crack growth by Eqs.(3) and (4).

Figure 11 presents the results of $\mathcal{E}_c(t, a)$ evaluated by Eqs.(3) and (4) based on Figs.9 and 10. Here, for $\mathcal{E}_c(t_0, a_0)$ in Eq.(3) the value for each initial crack length was used and for $(\partial \mathcal{E}_c/\partial a)_{unl}$ the value of $(\partial \mathcal{E}_c/\partial a)_{shear}$ for each specimen was used. The integral in Eq.(3) was evaluated from the third-order B-spline functions which interpolate the values of the integrand for a discrete growing crack length corresponding to the nodes of load-point-displacement. From the results in Fig.11, the following is found:

(i) The results of $\mathcal{E}_c(t, a)$ are independent of the initial crack length, and their changes seem to be peculiar to the specimen types. Further, the changes correspond to the changes in the shape of post-fracture surface, and their values become constant in the region of the crack growth accompanied with a uniform fracture mode.

Table 3 Evaluated results of $\mathcal{E}_{ctear}$ and $(\partial \mathcal{E}_c/\partial a)_{shear}$

THICKNESS	SECP		CCP	
	$\mathcal{E}_{c\,tear}$	$\frac{\partial \mathcal{E}_c}{\partial a}{}_{shear}$	$\mathcal{E}_{c\,tear}$	$\frac{\partial \mathcal{E}_c}{\partial a}{}_{shear}$
mm	KN/mm	KN/mm^2	KN/mm	KN/mm^2
2.0	0.041	0.012	0.040	0.016

Here, we express the constant values by $\mathcal{E}_{c\,shear}$. Table 4 shows the results for the two specimen types obtained as the averages of the values for each initial crack length. From the table, the following is found:

(ii) The values of $\mathcal{E}_{c\,shear}$ are approximately double those of $\mathcal{E}_{c\,tear}$ and those for CCP are slightly larger than those for SECP.

The tendency in (ii) corresponds to

NII-Electronic Library Service

The Japan Society of Mechanical Engineers

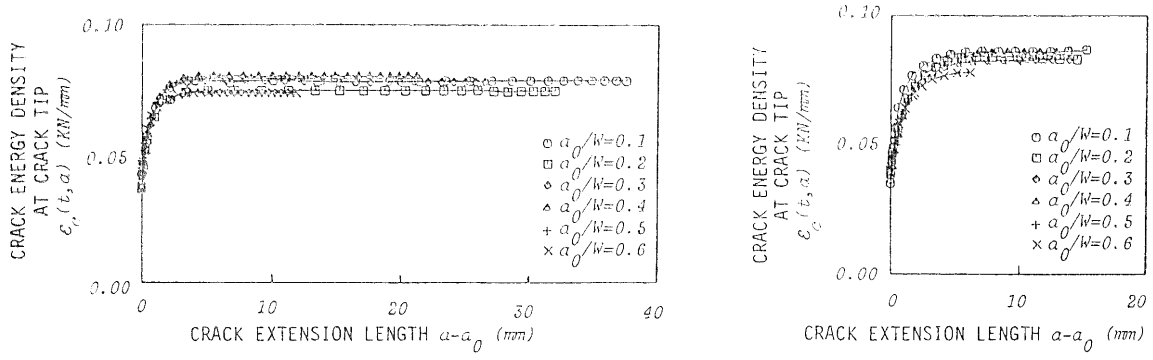

Fig.11 Crack energy densities at crack tip $\mathcal{E}_c(t, a)$ after onset of crack growth

that for $\partial\mathcal{E}_c/\partial a(t, a)$ and it is grasped in the same way as for $\partial\mathcal{E}_c/\partial a(t, a)$. Based on the results and considerations, it can be said that the change of $\mathcal{E}_c(t, a)$ characterizes the fracture resistance corresponding to the fracture mode from the onset of crack growth through the stable growth process.

5. Conclusions

In this Report, experiments of ductile crack stable growth of thin plate were carried out, and, based on the results, the fracture resistances by crack energy density were evaluated by the method proposed in the 1st Report. The results are as follows:

(1) The crack energy density at crack tip at onset of crack growth $\mathcal{E}_c(t_0, a_0)$ is independent of the initial crack length, and its value is peculiar to the fracture mode.

(2) The changes of the additional rate of crack energy density at growing crack tip $\partial\mathcal{E}_c/\partial a(t, a)$ and the crack energy density at growing crack tip are also independent of the shape of post-fracture surfaces. Further, in the stable crack growth under a uniform fracture mode mainly formed by shear fracture, the values become constant ones represented by $(\partial\mathcal{E}_c/\partial a)_{shear}$ and $\mathcal{E}_{c\,shear}$ shown in Tables 3 and 4.

(3) The values of $\mathcal{E}_{c\,tear}$, $(\partial\mathcal{E}_c/\partial a)_{shear}$ and $\mathcal{E}_{c\,shear}$ for SECP and CCP are approximately on the same levels respectively, although the latter two values for CCP are slightly larger than those for SECP corresponding to the differnece of the fracture mode.

Table 4 Evaluated results of $\mathcal{E}_{c\,shear}$

	SECP	CCP
THICKNESS	$\mathcal{E}_{c\,shear}$	$\mathcal{E}_{c\,shear}$
mm	KN/mm	KN/mm
2.0	0.077	0.084

Based on the results above, it can be said that the results of $\mathcal{E}_c(t_0, a_0)$, $\partial\mathcal{E}_c/\partial a(t, a)$ and $\mathcal{E}_c(t, a)$ characterize the fracture resistances of a material corresponding to the fracture modes and the evaluation of fracture resistance by the proposed method is valid and applicable.

References

(1) Watanabe, K., Bulletin of the JSME, 24-198 (1981), 2059.
(2) Watanabe, K., Bulletin of the JSME, 26-215 (1983), 747.
(3) Watanabe, K. & Azegami, H., Bulletin of the JSME, 29-257 (1986).
(4) FACOM FORTRAN SSL II MANUAL, (in Japanese), 79 SP-0050-5 (1980), 46, FUJITSU LIMITED.

NII-Electronic Library Service